Underway velocity measurements in Alderney Race: toward a 3D representation of tidal motions

Alexei Sentchev, Thinh Duc Nguyen, Lucille Furgerot, Pascal Bailly Du Bois

PHILOSOPHICAL TRANSACTIONS A

royalsocietypublishing.org/journal/rsta

Research

Cite this article: Sentchev A, Nguyen TD, Furgerot L, Bailly du Bois P. 2020 Underway velocity measurements in Alderney Race: toward a three-dimensional representation of tidal motions. *Phil. Trans. R. Soc. A* 20190491. http://dx.doi.org/10.1098/rsta.2019.0491

Accepted: 18 March 2020

One contribution of 13 to a theme issue 'New insights on tidal dynamics and tidal energy harvesting in the Alderney Race'.

Subject Areas:
oceanography, ocean engineering

Keywords:
acoustic Doppler current profiler measurements, Alderney Race, profile approximation, tidal current, velocity profile

Author for correspondence:
Alexei Sentchev
e-mail: alexei.sentchev@univ-littoral.fr

Underway velocity measurements in Alderney Race: toward a three-dimensional representation of tidal motions

Alexei Sentchev[1], Thinh Duc Nguyen[1,2], Lucille Furgerot[3] and Pascal Bailly du Bois[4]

[1]Laboratory of Oceanology and Geosciences, CNRS UMR 8187, University Littoral Côte d'Opale, Univ. Lille, Wimereux 62930, France
[2]Water-Environment-Oceanography Department, University of Science and Technology of Hanoi, and Institute of Oceanography VAST, Nha Trang, Vietnam
[3]LUSAC, Laboratoire Universitaire des Sciences Appliquées de Cherbourg, Universtiy Normandie, Cherbourg-en-Cotentin 50100, France
[4]IRSN/DEI/SECRE/LRC, Institut de Radioprotection et de Sûreté Nucléaire, Direction de l'Environnement et de l'Intervention, Laboratoire de Radioécologie de Cherbourg-Octeville, Cherbourg-en-Cotentin 50100, France

AS, 0000-0001-6971-9505; PBB, 0000-0001-8436-0772

Alderney Race, located northwest of the Cotentin Peninsular (France), is a site with high tidal-stream energy potential. Circulation through Alderney Race is complex, with current speed exceeding $3\,\mathrm{m\,s^{-1}}$ at neap tide. Towed acoustic Doppler current profiler (ADCP) measurements and static point velocity measurements were performed in July 2018 focusing on assessment of circulation and vertical structure of tidal currents. Transect surveys revealed peculiar features of local dynamics such as change in location of the tidal jet on ebb and flood flow. The spatial expanse of the tidal jet was quantified and regions with largely sheared or nearly homogeneous velocity distributions were identified on the cross-sections. Velocity profiles acquired along the cross-sections were accurately characterized using a power law. The spatial variability of the power-law exponent α was found large and correlated with the tidal

THE ROYAL SOCIETY PUBLISHING

conditions. The largest variation in profile shape was observed in the northern sector and assumed to be generated by the current interaction with a bathymetric constriction. The velocity profiles were found to vary from highly sheared on flood flow to nearly homogeneous on ebb flow, with corresponding range of power-law exponent α variation from 6 to 14. In the southern sector, over a relatively smooth bathymetry, the velocity profile shape was accurately approximated using the 1/7 power law with a range of variation of α from 6.5 to 8, with respect to the tidal conditions. To our knowledge, this is the largest field survey done using towed ADCP and the results could represent a significant advance in tidal site characterization and provide advanced information to turbine developers.

This article is part of the theme issue 'New insights on tidal dynamics and tidal energy harvesting in the Alderney Race'.

1. Introduction

In recent years, the tidal energy sector has been growing rapidly in interest as more countries look for ways to generate electricity without relying on fossil fuels. In comparison to other sources of renewable energy, tidal-stream energy has many perceived benefits, including the quality of electricity production because of its predictability (e.g. [1]) and the social acceptance level due to a reduced visual impact.

To be economically feasible, the tidal energy converters (TECs) require large current velocities: typically spring tide velocities in excess of 2.5 m s^{-1} [2]. Coastal areas with such highly energetic flow have limited size and are located in general in straits, passages between islands, or in the vicinity of headlands. The region of Channel Islands possesses several of such areas [3]. Alderney Race, located between the Cotentin Peninsula in France and Alderney Island (UK), is assumed to have the largest potential. This is relatively shallow water strait, 15 km large, with peak spring tide current velocities exceeding 5 m s^{-1}.

Although numerous modelling studies provided a realistic assessment of the local hydrodynamics (e.g. [3–7]), none of them focused on the identification of three-dimensional fine-scale features of tidal motions, such as tidal current jet location, its vertical expansion, velocity shear, its space and time variability. These features of local hydrodynamics are assumed to be of primary importance at the advanced stage of tidal-stream energy projects [8].

As the majority of TECs are designed to be located in the bottom boundary layer, a region where the flow experiences friction from the seabed, the knowledge of vertical shear of current velocity is a major consideration. It is assumed to have important implications for turbine efficiency and resilience (e.g. [9,10]) as well as for the instantaneous power available, as described in [11]. For this reason, TEC developers look for detailed characteristics of the flow speed across the area swept by the turbine blades and the velocity profile shape characterization is an important issue in the turbine performance research and in the planning stage of the projects (e.g. [12]).

Due to friction from the seabed the current velocity profile over shallow water, at depth suitable for TEC deployment (i.d. less than 50 m), has a nonlinear shape. At the beginning of the last century, Prandtl [13] and von Kármán [14] proposed formulations for velocity profile approximation in the boundary layer by the logarithmic and power law. Both approximations, valid for the layer above a thin roughness sub-layer, were extensively used in physical oceanography (e.g. [15–17]). The 1/7th power-law approximation is typically used to characterize the velocity profile in a tidal flow and resource assessment at tidal-stream energy sites (e.g. [18–20]). However, a number of factors, including the acceleration/deceleration of the tidal flow, wave-current interaction, seabed forms, etc. can cause deviations from the 1/7th power-law formulation. Lewis *et al.* [21] documented a large range of variation of the power-law exponent at sites in the Irish Sea. In particular, an extremely high shear in the tidal flow (i.e. 1/4th power-law profile shape) was observed which may have important implications for turbine

performance. A different parametrization (i.e. 1/10th power law) was suggested by O'Rourke *et al*. [22] who studied the tidal-stream resource around the Ireland. This was found in agreement with the North American Electric Power Research Institute Inc (EPRI) guidelines [19,23]. Large temporal variability of power-law exponent, reported at a prospective tidal power site in the Irish Sea [21,22], highlighted the necessity to improve understanding of the hydrodynamic processes which cause this variability.

In Alderney Race, due to extremely harsh flow conditions and difficulties of *in situ* data acquisition, high-quality velocity measurements are scanty and a detailed assessment of tidal flow conditions from direct measurements was not possible until recently. Bennis *et al*. [24] were among the first who analysed current velocities recorded by a bottom-mounted acoustic Doppler current profiler (ADCP) in Alderney Race. The ADCP data were used for estimating wave parameters and validating a three-dimensional hydrodynamic model coupled with a wave model. Velocity profiles for only eight specific time intervals, accounting for different wave conditions, were extracted from ADCP records and compared with the model outputs. Furgerot *et al*. [25] used longer velocity time series for assessing the wave effect on velocity profiles.

The present study extends the previous observational works and has two objectives. The first is focused on assessing the spatial variation in the velocity field over the study site and, in particular, the vertical variation of the horizontal velocity vector. This has been achieved by performing transect surveys by towed ADCP system allowing characterization and mapping of the flow field at large scale and from the surface to bottom.

The second objective aims to characterize the temporal variability of tidal current velocity profiles using both underway and static point velocity measurements. We employed methods, largely used in tidal energy research, to estimate the velocity profile shape by performing different formulations. Therefore, the suitability of characterizing the velocity profile by the power law or logarithmic law was evaluated in this study.

Our results bring new insights on the three-dimensional representation of the tidal stream and help in a better understanding of the physical process controlling the space–time variability of tidal currents. The acquired data offer a unique opportunity for evaluating the three-dimensional model performance in reconstructing the tidal flow and resource characterization. The data can also be used to assess different control strategies and to design a tidal current turbine to suit the site-specific characteristics.

2. Material and methods

(a) Study site

Velocity measurements presented here were performed in the eastern (French) sector of Alderney Race, northwest of the Cotentin Peninsula (figure 1). The surveys accomplished a long period of data acquisition, started in spring 2017. The surveyed area is approximately 10 × 7 km square with water depth less than 40 m in the majority of the domain and an abrupt increase of depth, to more than 60 m, in the northern sector (figure 1). This large fall of water depth is the major feature of local bathymetry. Another interesting feature, closely associated with the first, is the spatial variation in nature of the seabed, which has been documented in details by Furgerot *et al*. [26]. Both features constrain the velocity shear. The sea surface height (SSH) record in Goury, a small harbour close to the surveying area (see figure 1 for location) exhibits a wide range of tidal variations (2.5–7 m) predominantly semi-diurnal and globally symmetric. The current velocity on ebbing and flooding tide is not symmetric within the whole domain. The velocity asymmetry shows spatial variations within the range from 0.95 to 1.2 [27]. On average, current velocities are higher during ebb tide than during flood tide (asymmetry greater than 1). Peak flood and ebb-tidal velocities occur at high and low water, respectively, and the current reversal occurs at mid-tide. The tidal current dynamics is thus referred to as a progressive wave system. The tidal wave propagates northward during flood flow which lasts for 6 h and then changes a direction to southward for the next 6 h.

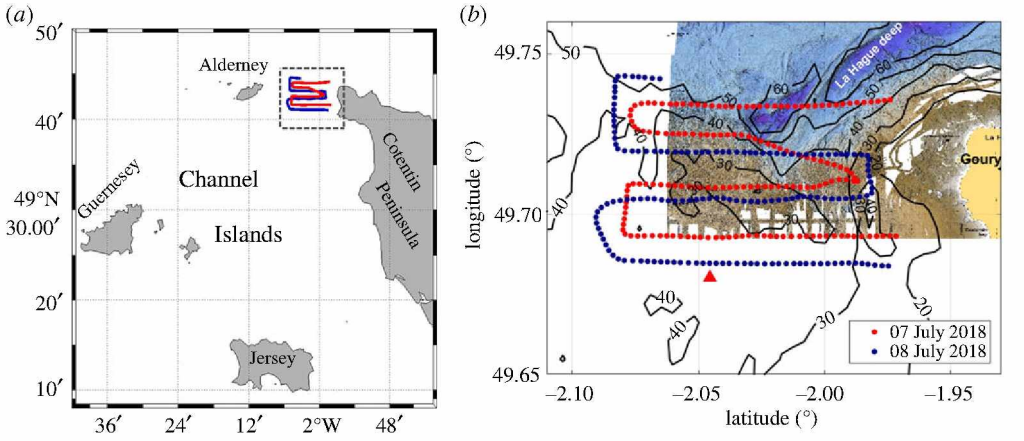

Figure 1. (*a*) Channel Islands region in the English Channel and study area (grey dashed rectangle) located between the northwest coast of Cotentin (France) and Alderney Island (UK). (*b*) High-resolution bathymetry map of Alderney Race (cf. [26]) with bathymetry contours (20, 30, 40, 50, 60 m) given in black, and two towed ADCP surveys in 2018. Surveys on 7 July 11.15–15.40 UTC (red) and on 8 July 06.30–10.50 UTC (blue) are used for detailed analysis of flood and ebb flow, respectively. Red triangle denotes the location of the bottom-mounted ADCP. Geographical names used in the text are also shown. (Online version in colour.)

Current speed variation during a fortnight cycle is also large. At neap tide, the maximum tidal current speed attains 3 m s^{-1}, in the eastern sector of Alderney Race, at a distance not exceeding 3 km off the French coast [28]. This is typically the result of topographic flow amplification. Spring tidal flow is much more powerful. According to modelling results, the highest velocities (more than 5 m s^{-1}) are found again in the eastern sector of Alderney Race on ebb tide, in a large area extending much further, up to 7 km, offshore (e.g. [3,28]).

(b) Static point velocity measurements

Static point velocity data were collected during 129 days, between 27 February and 6 July 2018, with an upward-looking 500 kHz broadband Teledyne ADCP V50. ADCP was mounted on an OPENHYDRO experimental platform sitting motionlessly on the seabed with depth 34 m at low tide. Seabed topography was relatively smooth at deployment site (49.6803 °N and −2.0455 °W) with a majority of cobbles and blocks with fixed fauna and possible corestones occupying the southern sector of the study area. The profiling range obtained was from 1 to 29 m above the seabed with 1-m vertical spacing. Velocity values in the surface 5 m thick layer were not considered in the analysis.

One-hour mean velocity profiles were derived from the along-beam velocities, acquired at 1 Hz. The statistical uncertainty in the mean velocity estimates, caused mainly by turbulent fluctuations, was considerably reduced by averaging (to less than 1% of the velocity value). The contribution from Doppler noise was negligible. A total of 15 days of data were processed. Following EMEC recommendations [29], only profiles with the depth average velocity exceeding 1 m s^{-1} were used in subsequent analysis. These represent 70% of the total dataset.

(c) Underway velocity measurements

Underway velocity measurements (i.e. velocity measurements throughout the water column in the Lagrangian frame by towed ADCP) were performed by using two experimental platforms deployed simultaneously: one—subsurface platform, carrying a broadband ADCP (600 kHz

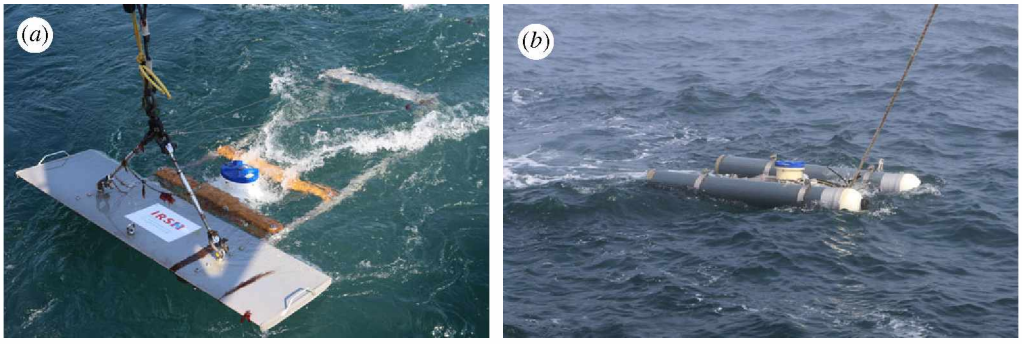

Figure 2. Experimental platform Dynalest carrying a 600 kHz RDI ADCP (*a*) and surface platform Koursk carrying a 1.2 MHz RDI ADCP (*b*), both towed by the R/V 'Côtes de la Manche' in Alderney Race. (Online version in colour.)

Teledyne WorkHorse Sentinel), and another—surface platform, carrying a 1.2 MHz Teledyne ADCP. Both platforms were towed by the R/V 'Côtes de la Manche'.

The deep-towed depressor platform 'Dynalest' is 2.4 m long and 1.6 m wide and was developed at the National Institute for Radiological Protection and Nuclear Safety (IRSN). It is composed, in the rear part, of an adjustable tail plane (with two vertical stabilization wings) and a main wing in the front part, connected together by two girders (figure 2*a*). The wing assures the maximum stability of the platform in a wide range of operational speeds (1–5 m s^{-1}) without generating tilts. The principal of operation of 'Dynalest' platform is described in detail by Bailly du Bois *et al*. [30]. During the surveys, the platform was located roughly 7 m below the water surface to avoid perturbations by the wake.

The second experimental platform 'Koursk', featuring two cylindrical hulls 1.80 m long and 0.2 m in diameter, connected by a 0.8 × 0.8 m stainless frame, was carrying a surface mounted ADCP (figure 2*b*). The distance from the boat central axis was controlled by an adjustable side fin allowing to avoid contamination by the wake of the boat. The ADCP's transducer head was located 0.3 m below the water surface The blanking was set to 0.4 m, the bin size to 0.5 m and the centre of the first bin was roughly at 1 m below the water surface. The velocity profiles were acquired in the surface 15 m thick layer.

Both ADCPs were set to operate at the pinging rate of 1 Hz, providing a velocity error of 0.07 m s^{-1} (according to Teledyne software). Single-ping bottom tracking enabled to correct for boat's movement and the recorded velocities formed a current vector in the fixed frame relative to the bottom. The ADCP data were merged with navigation data provided by the onboard GPS system also operating at 1 Hz.

Several towed ADCP surveys were performed. The results of the two longest surveys, separated by 1.5 tidal cycles are presented in this paper. Survey S1 was performed on 7 July 2018 at 11.15–15.40 UTC, during flood tide. Survey S2, targeting ebb tide, was performed on 8 July 2018 at 06.30–10.50 UTC. Thus most of the flood and ebb flow periods were covered by observations. The survey tracks are shown in figure 1.

Current velocities recorded by ADCPs were corrected for boat motion and averaged within 1 min intervals. GPS coordinates were also sub-sampled every minute, so that the distance between the thinned along-track data points varied within 120–180 m, depending on the towing speed. Velocity profiles derived from two instruments, overlapping within 8–15 m depth layer, were merged and the resulting profiles, at 1 min spacing, extended from the surface (starting 1 m below the sea surface) to near bottom.

Towed ADCP surveys were performed during the neap tide, specifically targeted for recovering of two bottom-mounted ADCPs, taking video of the seabed, and sampling sediments in the study area. Weather conditions were very good with the weak wind (max speed 5 m s^{-1}) and low waves (Hs < 0.4 m).

(d) Methods of velocity profile approximation

Two major methods (two groups of methods) are currently used for velocity profile approximation. They employ either a logarithmic or power-law approximation. The first, the logarithmic approximation, uses the basic physics of the boundary layer dynamics proposed by Prandtl [13], further developed by von Kármán [14] and generalized by Monin & Obukhov [31] for the atmospheric boundary layer. The theory stands that in the boundary layer, above the roughness sub-layer, where molecular viscosity and underlying surface roughness are important, the flow velocity U at altitude z above the underlying surface is given by

$$U(z) = \frac{u^*}{k}\left(\ln\left(\frac{z}{z_0}\right) - \psi\left(\frac{z}{L}\right)\right), \tag{2.1}$$

where u^* is the friction velocity, k is von Kármán constant ($k = 0.4$) and z_0 is the surface roughness.

The general form of equation (2.1) contains universal functions $\psi(z/L)$ accounting for the stability of the boundary layer. L is known as the Monin–Obukhov length scale. Functions Ψ are not used for assessing the profile evolution in the ocean bottom boundary layer, thus simplifying the expression for velocity. Velocity U is thought to be the ensemble average velocity, i.e. averaged sufficiently to eliminate turbulent fluctuations, and the equation (2.1) has the practical advantage of describing only the mean velocity profile. At level z_b above the bottom, where the current measurements are performed, the multiplier u^*/k can be written as follows:

$$\frac{u^*}{k} = \frac{U_b}{\ln(z_b/z_0)}.$$

Introducing it into (2.1) yields the expression for velocity profile approximation with respect to a reference velocity U_b at z_b:

$$U(z) = U_b \cdot \frac{\ln(z/z_0)}{\ln(z_b/z_0)}. \tag{2.2}$$

This approximation can be very effective for specific conditions or regions. But it has two weak points. The first is the difficulty in roughness z_0 estimation and the second is the altitude z_b at which the reference velocity is prescribed. Both quantities may have optimal values allowing to minimize the error of approximation. But these values may vary at a wide range with respect to the flow strength thus limiting the large scale use of the logarithmic law.

For this reason, another method of approximation, more simple in use, is employed for reconstructing the velocity profile with respect to velocity U_0 in the surface ocean layer, or velocity U_m at the mid-depth (or another level), sometimes more accessible for measurements (cf. [20]):

$$U(z) = U_0\left(\frac{z}{h}\right)^{1/\alpha}. \tag{2.3}$$

The power coefficient α is defined empirically and can strongly depend on the bottom roughness, stratification and velocity range. The most frequently used value of α is 7. It was suggested for the first time by von Karman [32] for a relatively smooth underlying surface. This expression is customary used in oceanographic studies (e.g. [19]) and in the wind energy industry (e.g. [33]).

Equation (2.3) can take another form which is also largely used by oceanographers:

$$U(z) = \bar{U}\left(\frac{z}{\beta h}\right)^{1/\alpha}, \tag{2.4}$$

with bed roughness coefficient β, vertically averaged velocity $\bar{U}$ and the water depth h. This formulation, proposed by Soulsby [17] on the basis of experiments in flume tank and *in situ* measurements, is adopted by the tidal energy community for characterizing the technically exploitable resource at prospective sites (e.g. [21,34]). Bed roughness coefficient β is related directly to grain size of seabed sediments and can vary in a large range. The value 0.32 (corresponding to 0.32×10^{-3} m) was suggested initially by Soulsby [17], but larger value (0.40 for example) may be used as adjustable parameter allowing the best fit of velocity profile to

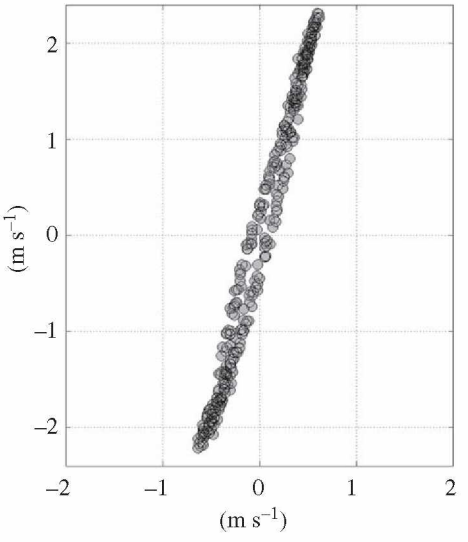

Figure 3. Tidal current ellipse from bottom-mounted ADCP measurements during a fortnightly cycle from 22 June 2018 to 7 July 2018. Current velocities were depth averaged and hourly averaged.

real data. The fitting of measured velocity profiles to the power law form (2.4) is performed in a least-squares sense after linearizing equation (2.4) by log function. The resulting power-law coefficient α provides the minimum approximation error for a given value of β, which was also varied iteratively in the range 0.005–0.5.

3. Results

(a) Static point velocity measurements and profiles

At the bottom-mounted ADCP location (figure 1), the current velocity vector evolution during a tidal cycle describes an ellipse. Figure 3 shows the depth-averaged current velocities for the 15-days period. The shape of the ellipse does not change with depth and, on average, the flow direction at different depths levels was very steady. The mean velocity on ebb and flood tide is nearly the same (approx. $1.4\,\mathrm{m\,s^{-1}}$), the velocity asymmetry is 1.02 revealing that flood and ebb flow are almost in equilibrium. The streamwise direction was found to be aligned with bathymetry contours. The ellipse major axis is rotated clockwise by 20° with respect to the North, and the ratio of the mean spanwise to streamwise component (ellipticity) is 0.05.

Hourly averaged velocity profiles (figure 4) were analysed for different stages of the tidal cycle: peak velocity period, flood and ebb flow at neap and spring tide. After the least-squares fit, individual profiles were found to follow the $1/\alpha$ power law with the exponent α ranging from 5 to 10.8, with more uniform spreading within the range $5 < \alpha < 9$ for both neap and spring tide conditions (figure 5). For the whole period, the mean α was equal to 7.0, with slightly larger mean value obtained for neap tide and smaller for spring tide ($\alpha = 6.9$). These mean estimates suggest that the velocity profile shape does not change much during the whole fortnight period and uniform spreading evidences the absence of correlation with flow speed. The standard deviation of α estimates is close to 1 (1.1 and 1.2 for spring and neap tide stages, respectively). The optimal value of the bottom roughness coefficient was found to be 0.4. To further assess variations in velocity profile shape, time averaging of current velocities was performed for multiple 1-h periods encompassing the largest (peak) velocity: 1-h interval centred on the peak velocity and periods preceding and following the peak velocity time, spaced by 1 and 2 h from the peak flow

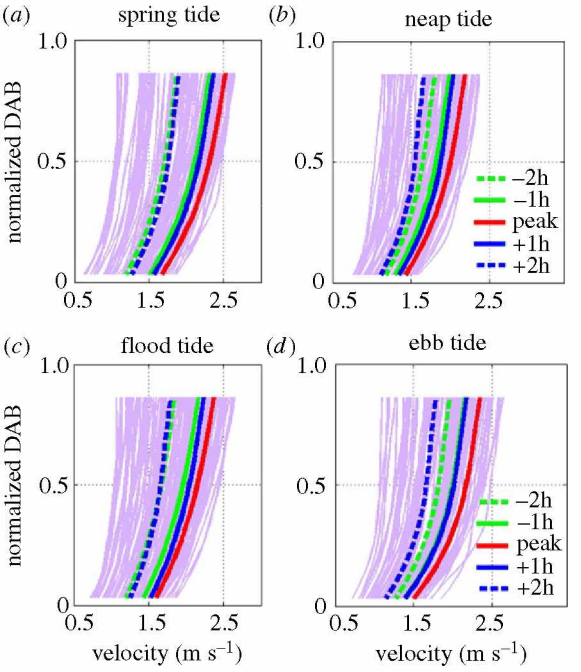

Figure 4. Current velocity profiles during spring/neap tide (*a*,*b*) and flood/ebb tide (*c*,*d*) from bottom-mounted ADCP measurements in Alderney Race. The mean velocity profile during the peak current is shown in red (multiple 1 h averaging periods are centred on peak velocity). One hour averaged velocity profile corresponding to observation period 1 and 2 h before/after the peak velocity are given in green/blue solid and dashed lines, respectively. Initial velocity profiles recorded by ADCP, 60 min averaged, are given in purple. (Online version in colour.)

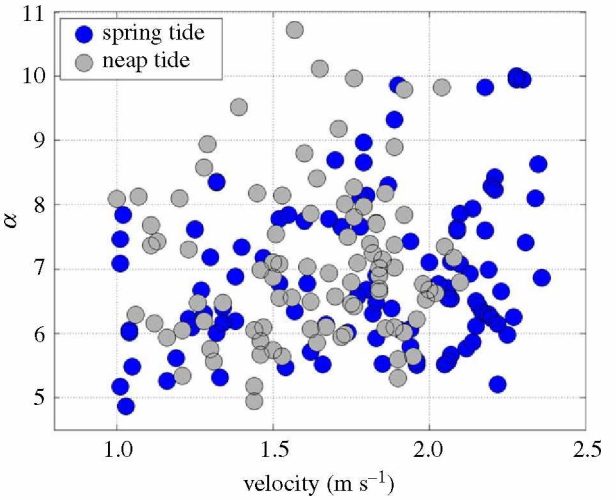

Figure 5. Values of power-law exponent α versus depth-averaged velocity $\bar{U}$ for spring and neap tide conditions. (Online version in colour.)

time interval. The resulting 5-h interval covers the most energetic ebb and flood flow and the corresponding mean profiles are shown in figure 4.

The results, summarized in table 1, show that for both ebb and flood flow the power-law exponent does not change much: α varies from 6.5 to 8 with the values slightly smaller than 7

Table 1. Values of the power coefficient α estimated from the best fit of the velocity profiles from BM ADCP and averaged over five selected periods (peak flow, 1 and 2 h preceding and following the peak flow) for different tidal stages: ebb and flood flow, neap and spring tide. Numbers in brackets match the relative error of approximation (%).

period of analysis		peak—2 h	peak—1 h	peak vel.	peak + 1 h	peak + 2 h
27 June to 3 July 22–24 June and 4–6 July 2018	α_{spring}	6.4 (1%)	6.7 (1%)	6.9 (1%)	6.9 (1%)	7.2 (<1%)
	α_{neap}	6.7 (1%)	6.7 (1%)	6.7 (1%)	7.0 (1%)	7.4 (<1%)
22 June to 7 July 2018	α_{flood}	6.5 (1%)	6.7 (1.4%)	6.9 (1%)	7.3 (1%)	8.0 (<1%)
	α_{ebb}	6.8 (1%)	6.7 (1%)	6.6 (1%)	6.6 (1%)	7.0 (1%)

for peak velocity flow. The relative error of profile approximation is very low approximately 1% (shown in brackets in table 1). Similar mean values of α and the range of variation are found for neap and spring tide conditions suggesting no correlation between the peak flow speed and profile shape, as shown in figure 5. This allows to conclude that, in the static ADCP location, where less energetic tidal stream occurs, the velocity distribution during the strongest flow could be approximated by 1/7 power law with relatively high accuracy. Two hours after the peak flow, while the tidal-stream weakens, the velocity profile becomes slightly less sheared ($\alpha = 8$) (table 1 last column).

An attempt was made to perform an approximation of time-averaged velocity profiles using equation (2.3) for logarithmic law (results not shown). The reference velocity U_b recorded at 2 m above the bottom was used ($z_b = 2$ m). This gives the best approximation with the resulting error approximately 1–2.5% which is slightly larger than that obtained for the power-law approximation (1–1.4%, table 1). In this analysis, the bottom roughness z_0 was varied in a wide range, from 0.00005 to 0.00030 m, to obtain this best fit to measurements. The optimal value of z_0 was found to be 0.00025 m for ebb flow providing an accurate approximation of profiles for this tidal stage with low error (approx. 1%). The accuracy of approximation was found to be very sensitive to the value of z_0 used.

(b) Underway velocity measurements

Towed ADCP survey enables the characterization of space–time variations of tidal currents. Figure 6*a*,*b* show velocity recorded along the track during flood and ebb flow survey after depth and time averaging within 1 min intervals. Each survey lasted more than 4 h and covered the period of fully developed flow (velocity close to 3 m s^{-1}) as well as a part of the tidal cycle before and after the current reversal (velocity less than 1 m s^{-1}).

Spatial distribution of underway velocity measurements on flood and ebb tide is given in figure 6*c*,*d* (only one of two vectors is plotted). Results of current mapping are superimposed on modelled fields corresponding to the mid-time of each survey. This helps in the interpretation of the observed velocities. The model used is a largely validated two-dimensional local circulation model MARS (e.g. [5]). Vector current maps reveal some characteristic features of tidal dynamics in Alderney Race such as the location of tidal jet and its spatial expansion. During the ebb flow, the area of high-speed current is found at larger distance from the shore and the flow speed attains 2.5 m s^{-1} in a broad zone spread by more than 5 km (Figure 6*d*). Flood flow velocity is also large (3 m s^{-1}) but the current jet location is closer to the shore. This is the result of current convergence which is clearly seen in the model velocity field (figure 6*c*).

Velocity on cross-sections (figure 7) allows to characterize the spatial expansion of the tidal stream with depth and with respect to distance from shore. The velocity distribution with depth is nearly homogeneous for low current speed, observed both offshore and close to the shore on ebb tide (figure 7*b*). In the central part of the cross-section, the powerful tidal stream is seen to occupy

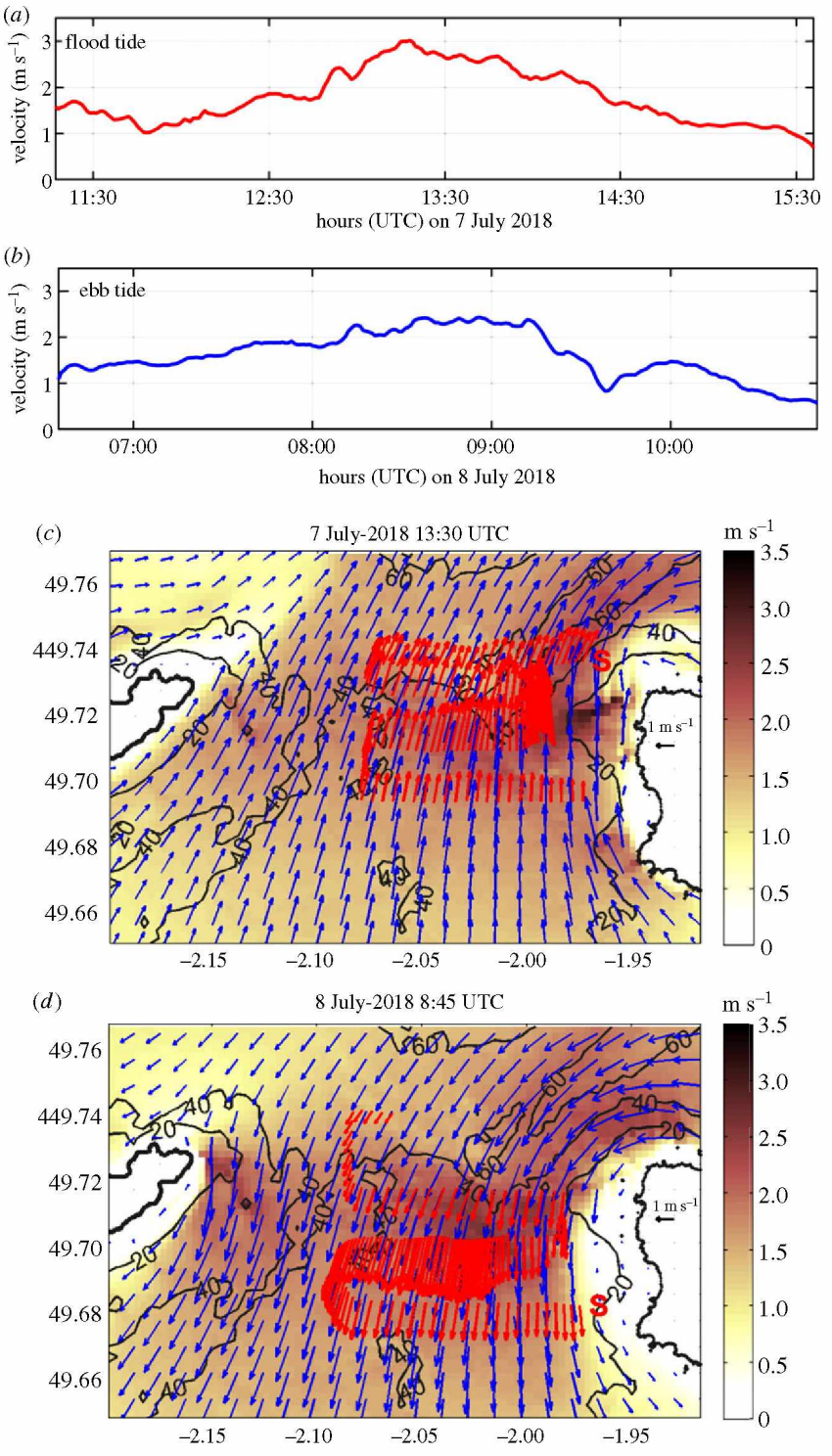

Figure 6. Vertically averaged and 1-min averaged current velocities along the track during the flood tide survey on 7 July, 11.15–15.40 UTC (*a*) and ebb tide survey on 8 July, 06.30–10.50 UTC (*b*). Current velocity vector maps from towed ADCP surveys (red vectors) on flood (*c*) and ebb tide (*d*). Modelled velocities (blue vectors) and velocity magnitude (background shading) are given for mid-time of each surveyed period. Letter S shows the starting point of each survey. (Online version in colour.)

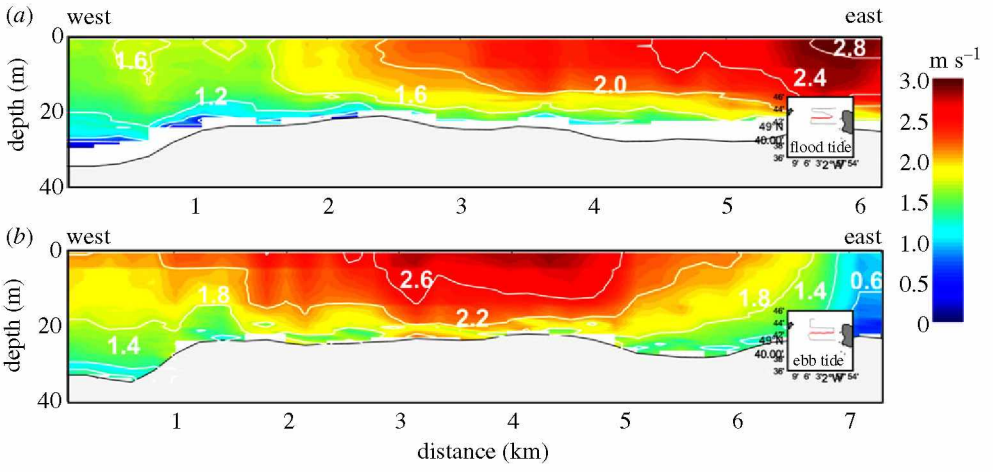

Figure 7. Current speed (1-min averaged data) along the cross-sections on flood tide (*a*) and ebb tide (*b*). The cross-section location is given in red in the insert. (Online version in colour.)

nearly the whole water column with velocities larger than 2 m s^{-1} in the surface 20 m thick layer (nearly homogeneous) while the total depth is approximately 25 m (between tick marks 2 and 5 km in figure 7*b*). Flood tide flow is more sheared over the cross-section and larger velocities (greater than 2.4 m s^{-1}) are observed close to the shore. An important feature of the velocity distribution is the increase of current speed over low depth (less than 25 m) thus evidencing the flow enhancement by local topography.

(c) Velocity profiles from underway acoustic Doppler current profiler measurements

Towed ADCP surveys in July 2018 gave us an opportunity to characterize the velocity distribution in the whole water column (from 1 m below the sea surface to bottom). Velocity profiles retrieved from measurements by two ADCPs were time averaged and merged, thus generating profiles with high spatial resolution along the track: 150–200 m. This resolution corresponded to the vessel's displacement during 1–2 min. Space averaging within 200 m was adopted for further assessment of the profile shape and their spatial variability. The mean profiles were approximated by the power law (equation (2.4)) and the resulting values of α are shown in figure 8. The power-law exponent was estimated with the constant roughness $\beta = 0.4$, which has proved to be the best approximation of profiles recorded by BM ADCP. Only profiles with depth-averaged velocity larger than 1 m s^{-1} were analysed. This explains the absence of data at the end of ebb flow survey and also over deep water, in the northern sector.

The largest variability of α was found during the ebb tide. Spatial patterns of α distribution look different for two tidal stages. Bathymetry gradients in the northern sector of the surveyed area appear to have a great influence on the velocity profile shape but only on ebb tide. Values of α range from less than 5 to more than 13 along the northern track (figure 8*b*). Large values of α (homogeneous velocity profiles) are observed in deep water (depth larger than 40 m), lower values (sheared profiles) in more shallow water. Topographic obstruction visible in the middle of the second cross-section of ebb tide survey (figure 7*b*) causes the flow acceleration and the velocity profiles appear more sheared ($\alpha < 7$), compared to highly homogeneous profiles ($\alpha > 13$) on the northern cross-section (figure 8*b*). Thus on ebb tide, over a short distance (2 km from North to South), the shape of velocity profiles changes from nearly homogeneous to largely sheared and the corresponding α varies from 5 to 14. This is the effect of large scale bathymetric feature: after the La Hague deep, the seabed rises up to a shallow water plateau (figure 1 for details).

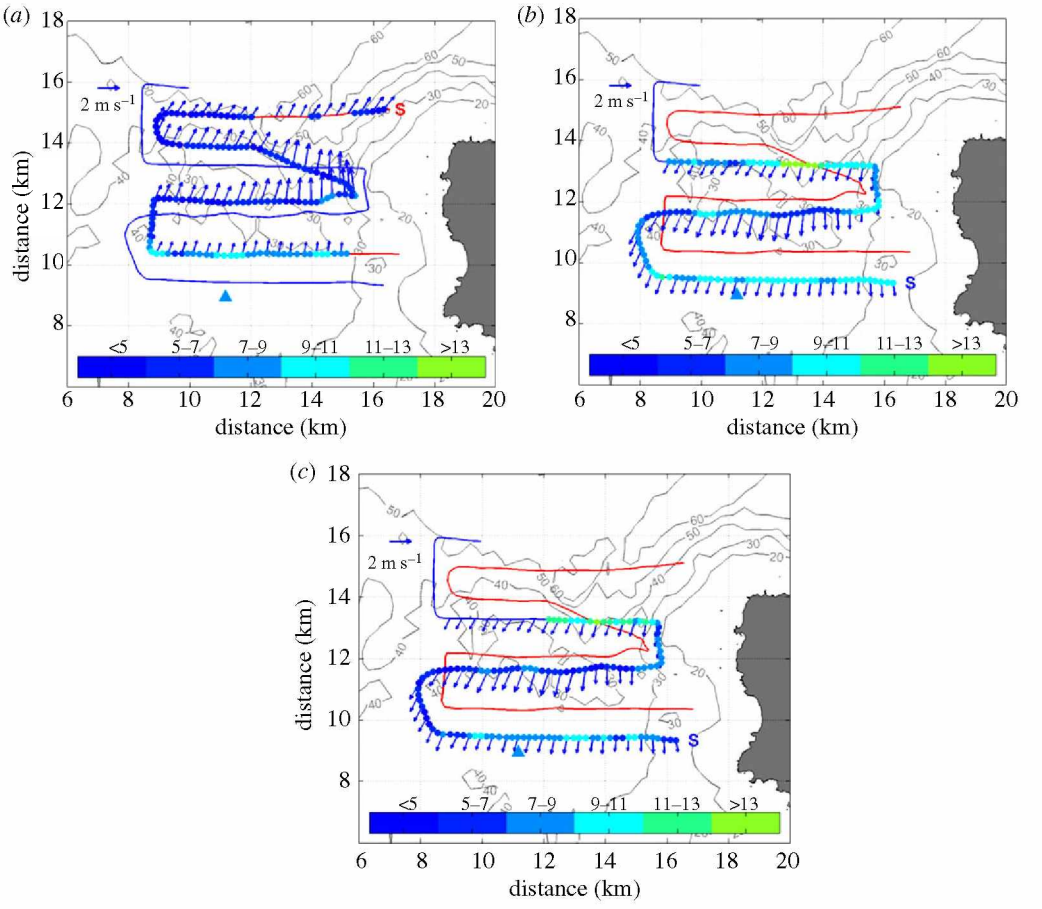

Figure 8. Current velocity vectors (blue) and power-law exponent α (colour shading) from velocity profile fit for flood tide (*a*) and ebb tide (*b*,*c*) conditions. ADCP derived profiles were averaged within 200-m bins along the track. In (*c*), the velocity profile fit was performed in the lower part of the water column extended to 25 m above the seabed. Letter S shows the starting point of each survey. The triangle shows the location of the BM ADCP. Face colour corresponds to α fit of the velocity profile from BM ADCP at time when the towed ADCP was nearby the BM ADCP location. (Online version in colour.)

On flood tide, the velocity distribution in the incident northward flow does not experience a notable influence of increasing depth. Velocity profiles appear sheared ($\alpha < 7$) over the majority of the area covered by ADCP measurements (figure 8*a*). In the southern sector, characterized by more smooth bathymetry, α variations are small, ranging from 7 to 11 for both ebb and flood flow.

As depth variation is large within the study area, it appears worthwhile to assess also the profile shape variability in the lower part of the water column whose vertical extension exceeds slightly typical size of bottom-mounted tidal stream devices. The upper limit of the layer was fixed to 25 m above bottom which is suitable for deployment and operation of large size devices such as OPEN-HYDRO-DCNS or SIMEC Atlantis devices, which hub height is located at a fixed distance above the sea bed. The resulting distribution of α is shown in figure 8*c*. The figure confirms that in the lower layer the velocity profile shape also experiences large spatial variability during ebbing tide. In particular, a rapid decrease of depth (from 60 to 40 m) in the northern sector and turbulence, resulting from the interaction of incident current with bathymetry, lead to homogenization of velocity profile there ($\alpha > 13$). Estimates of α in the western part of the northern cross-section in figure 8*c* are absent because the depth-averaged velocity is less than

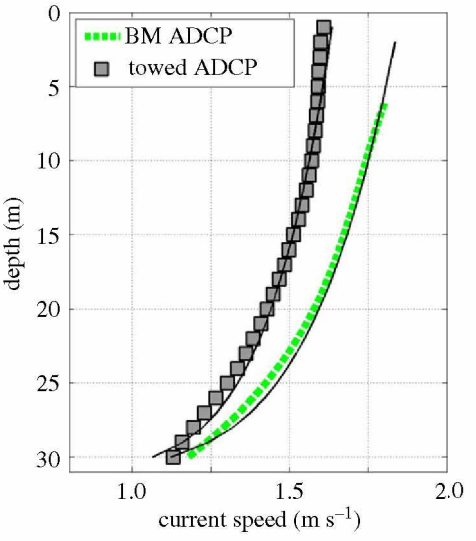

Figure 9. Velocity profiles derived from the bottom-mounted ADCP (green dashed line) and towed ADCP (grey squares) for the time interval when the vessel was nearby the BM ADCP location. Black lines are power law fit to data. The location of the bottom-mounted ADCP is given in figure 8. (Online version in colour.) Q7

1 m s^{-1} there. During flood tide, the spatial distribution of α in the whole water column and in the 25-m thick lower layer is similar (results not shown).

In order to further assess the accuracy of velocity profile approximation from towed ADCP measurements, a comparison was done with independent data—velocity measurements by the bottom-mounted ADCP. A fraction of the current record was selected when the towed ADCP was nearby the bottom-mounted ADCP (see figure 8 for location). The shortest distance between two ADCPs was approximately 500 m during the ebb tide survey, on 8 July. The BM ADCP was recovered in the morning on 7 July, two tidal cycles before the ebb tide survey, thus preventing synchronize data comparison. The mean profile acquired by BM ADCP 2 h before peak current (ebb tide conditions) is compared with a space–time averaged profile from a towed survey in the location closest to BM ADCP, also 2 h before peak current. The profiles are shown in figure 9. They follow the power law with the exponent $\alpha = 7$ for BM ADCP (table 1 first column, bottom line) and $\alpha = 8$ for towed ADCP, in this particular location with relatively flat bathymetry. Underway velocity measurements were averaged during 3-min interval corresponding to a distance of approximately 0.5 km.

The visual comparison allows to quantify the difference between two profiles. Good consistency is found for ebb flow profiles with the mean difference less than 0.2 m s^{-1}. This result is very encouraging as it shows the capability of the towed ADCP system to generate velocity profiles from underway measurements with relatively high accuracy level. An attempt was done to include into comparison a profile corresponding to neap flood tide conditions (mean profile, 2 h after the peak flow). On 7 July, the distance between ADCPs was larger, approximately 1 km, and the depth was lower. After averaging the towed ADCP velocities, the power-law approximation provided $\alpha = 9.5$ (figure 8*a*).

4. Discussion

Due to the growing interest in tidal energy conversion technique in many countries [22,35,36] a detailed assessment of the available resource is required to determine the commercial viability of any project prior to device deployment. At the initial stage, developers look for detailed characteristics of the flow speed across the area swept by the turbine blades. While a typical size

of TECs at demonstration sites approaches more than a half of the water depth, vertical shear in tidal flow is a major consideration in the planning stage of the projects.

Over the last decade, standardized methods of field data acquisition for resource characterization at tidal-stream energy sites have been proposed (e.g. [29,37]). Current measurements by ADCPs are routinely used to directly characterize the tidal flow. A bottom-mounted ADCP is often deployed for measuring temporal variations (e.g. [21,38,39]), while a vessel-mounted ADCP can measure spatial variations [8,40,41].

Thiébaut *et al*. [42] analysed the velocity data recorded by a bottom-mounted ADCP deployed in Aldernney Race, 4 km west off the Cotentin Peninsular (latitude of Goury in figure 1), for assessing parameters of the turbulence in the tidal flow. It was argued that below the surface layer affected by wave motions, the velocity shear is probably the major parameter controlling the evolution of turbulence in the water column. For this reason, the velocity shear in a tidal stream is of primary importance. Static point ADCP measurements performed recently at prospective tidal-stream energy sites (e.g. [20,21,43]) revealed that the velocity profile shape can be accurately approximated using a 1/7 power law. This formulation, proposed by Soulsby [17] on the basis of experiments in flume tank and *in situ* measurements, is adopted by the tidal energy community for characterizing the technically exploitable resource (e.g. [18,44]). Velocity profiles from the bottom-mounted ADCP deployed in Alderney Race, over a relatively smooth bathymetry, confirmed this property of velocity distribution. The mean value of power-law exponent, controlling the profile shape, was found to vary from 6.5 to 8 during the spring-neap tidal cycle, whereas the individual profiles (hourly averaged) revealed larger range of variation: from 5 to 10 (figure 5 and table 1). It should be highlighted that a highly sheared tidal flow (i.e. $\alpha \sim 5$), observed at likely operating times of turbines ($U > 1\,\mathrm{m\,s^{-1}}$), has important implications for TEC performance and resilience [45,46]. Thus, studies of the impact of highly sheared flow on different components of TECs, such as the blades and support structures, experiencing significant fatigue cycles during operation are of great importance (e.g. [47,48]). A better understanding of turbine-scale interaction with a turbulent and sheared flow is a key goal for successful operation and maintenance strategies at tidal energy sites.

The large variability of power-law exponent α was reported by Lewis *et al*. [21] at a prospective tidal power site in the Irish Sea. Their study and the present observations highlight the necessity to improve understanding of the hydrodynamic processes which cause this variability and interaction (e.g. [49]). In the Irish Sea, a significant correlation was found between the temporal variability of the power-law exponent and the tidal conditions. The velocity profile in accelerating flow during the flood tide was found more sheared whereas more homogeneous profiles characterized ebbing tide. The homogenization of velocity profile was assumed to be related to the influence of turbulence, locally generated by bathymetric features.

Another physical process controlling the velocity profile shape is wave motions and wave-current interaction. Assessment of local hydrodynamics in Alderney Race using a coupled three-dimensional circulation model and wave model was performed by Bennis *et al*. [24]. Modelled velocity profiles for eight specific time intervals, accounting for different wave conditions, were analysed and compared to ADCP records. The comparison revealed a significant effect of waves on profile shape, in particular, the velocity decrease in the upper layer (larger α) due to Stokes drift. At the same time, the authors highlighted difficulties in interpreting the model results due to (i) nearly orthogonal angle between the direction of incident waves and tidal current, (ii) phase lag between accelerating currents with and without waves and (iii) high level of turbulent motions with horizontal scales sometimes exceeding the water depth, not accurately reproduce in model simulations. The results reported by Bennis *et al*. [24] and by Lewis *et al*. [21,49] emphasized the importance of wave forcing on the current velocity profile.

Observations performed in Alderney Race in July 2018 were focused on assessing the spatial variability of the velocity field by performing transect surveys by towed ADCP system allowing characterization and mapping the flow field at large scale (site scale) and from the surface to bottom. It was demonstrated that on ebb tide, the incident flow, guided by the La Hague deep (greater than 60 m) (see figure 1 for location), appears in the middle of the Alderney Race. During

the flood tide, due to bathymetric constrictions in the eastern sector of Alderney Race, stronger flow occurs near the French shore. Spatial expansion of the tidal jet was characterized in each case. In this, we fully met EMEC's recommendations to carry out transect surveys by towed ADCP in order to assess the spatial variation in the velocity field over the site [29].

It is worth to mention that EMEC recommends to perform individual ADCP transects in less than 10 min, in order to avoid significant changes in the flow conditions during the survey. But this greatly limits the extent of the surveyed area (by about 1–1.5 km). Underway velocity measurements, used in this work, lasted more than 4 h for flood and ebb tide stages. Obviously, these measurements contain information on both spatial and temporal variations of tidal currents. These variations need to be separated from each other. A number of techniques allowing this separation have been developed. Goddijn-Murphy *et al.* [40] showed that if a tidal hydrodynamic model provides a reasonable estimate of flow field, an output of the model could be used to project the transect data to different time intervals of the survey. Using a two-dimensional model, they performed a reasonably accurate synchronization of the velocity data to the mid-survey time. More recently, Thiebaut *et al.* [28] employed the optimal interpolation (OI) technique for reconstructing space–time evolution of the velocity field derived from towed ADCP surveys in Alderney Race in 2017. The OI was initially applied by Sentchev and Yaremchuk [50] for underway velocity data processing at the local scale (Boulogne harbour in the English Channel). Then it was successfully used in Alderney Race allowing to improve considerably the quality of tidal-stream resource assessment there [28]. The data from the field surveys in July 2018, used in the present study, were also reprocessed by OI method recently [51].

The velocity profiles acquired along the cross-sections during flood and ebb tide were accurately characterized using the power law. The spatial variability of the power-law exponent α was found to correlate with the tidal conditions. In the northern sector of Alderney Race, close to bathymetric constriction (i.e. bathymetry change from 60 to 40 m), the shape of velocity profile and values of α revealed the largest variation: from highly sheared velocity profile on flood flow ($\alpha \approx 6$) to nearly homogeneous velocity distribution on ebb flow ($\alpha \approx 14$). This large variation of profile shape is not due to the influence of local-scale bathymetric features but results from the current structure modification by bathymetry gradients at large scale, upstream the measurement location. Bathymetric incisions, in the central part of the study area and in the western sector, control the flow direction on ebb tide while the steep increase of depth causes the flow acceleration and generates strong turbulence. Thiebaut *et al.* [42] have demonstrated that in this particular location, the horizontal scale of turbulent eddies (integral scale of turbulence) can exceed two or three times the local depth. Powerful turbulent motions and mixing are assumed to be the major factors affecting the ebb tide flow and generating nearly homogeneous velocity distribution on ebbing tide. On flood tide, the bottom friction over low depth (less than 40 m) affects the tidal-stream differently and generates velocity shear in the majority of Alderney Race. The values of power-law exponent α do not exceed 7 there. So strong space–time variability of the velocity profiles, occurring during a tidal cycle, and its spatial representation was not previously reported in publications, to the best of our knowledge. Hence, developers should be aware of fine-scale spatial variations of the tidal stream that may exist at potential tidal-stream energy sites. This suggests that detailed site surveys are essential at an early stage of resource characterization.

5. Conclusion

Transect surveys by towed ADCP were carried out in Alderney Race in order to assess the spatial variation of the velocity field over the site. The surveys revealed specific features of local tidal dynamics such as more faraway location of the tidal jet on ebb rather than on flood flow. Spatial expansion of the tidal jet was quantified and regions with largely sheared or nearly homogeneous velocity distribution were identified on the cross-sections. A combination of the high-resolution bathymetry map with underway velocity measurements allowed to provide a meaningful interpretation of the tidal jet location and to demonstrate a significant role of large scale bathymetric features affecting the flow. In particular, we demonstrated the role played by

the La Hague deep and the adjacent shallow water plateau in constraining the current direction and homogenizing the velocity distribution throughout the water column by turbulent mixing.

Velocity profiles acquired along the cross-sections during flood and ebb tide were accurately characterized using the power law. Maps of the power-law exponent distribution revealed that spatial variability of the flow field was as large as temporal variability. Large-scale bathymetric features and resulting turbulent motions generate velocity shear which is highly complex and has distinct spatial patterns. In the northern sector of Alderney Race, velocity profiles vary from highly sheared on peak flood flow to nearly homogeneous on peak ebb flow, with corresponding range of power-law exponent variation from 6 to 14.

Moreover, our results demonstrated that over a relatively smooth bathymetry, the mean velocity profile shape could be properly approximated using the 1/7 power law with a range of variation of power-law exponent α from 6.5 to 8, with respect to the tidal conditions. Our observations appeared to be in close agreement with the results reported in previous studies at prospective tidal sites. They confirm the relevance of the approach adopted by the tidal-stream energy community for characterizing the technically exploitable resource.

The towed ADCP survey proved to be efficient for tidal site characterization and be capable of overachieving requirements set by the EMEC guidelines, since the underway velocity measurements allowed assessing both spatial and temporal variability of the velocity field.

Finally, it was demonstrated in previous studies by the authors that merging high-resolution underway velocity measurements with modelling makes the tidal-stream estimation more accurate, compared to what the model can do alone. It offers a real opportunity for monitoring coastal currents at sites with large spatial extension and appears complementary to static point ADCP measurements.

Data accessibility. All the data acquired in the project will be available to the reader from July 2020 onwards. This data will be available via: http://www.geoceano.fr/programmes/anr-hyd2m.

Authors' contributions. A.S.: data acquisition and analysis, writing, correction of the ms. T.D.N.: data processing and analysis. L.F.: data processing. P.B.d.B.: data acquisition, modelling, revision.

Competing interests. We declare we have no competing interests.

Acknowledgements. This work benefitted from the funding support from France Energies Marines and the French Government, operated by the National Research Agency under the Investments for the Future programme: Reference ANR-10-IEED-0006-07. The study represents a contribution to the project HYD2M of the above programme. We would like to acknowledge the head of the research project, Anne-Claire Bennis (UNICAEN), the skipper and the crew of the R/V 'Côtes de la Manche'.

References

1. Lewis M *et al.* 2019 Power variability of tidal-stream energy and implications for electricity supply. *Energy* **183**, 1061–1074. (doi:10.1016/j.energy.2019.06.181)
2. Lewis M, Neill SP, Robins PE, Hashemi MR. 2015 Resource assessment for future generations of tidal-stream energy arrays. *Energy* **83**, 403–415. (doi:10.1016/j.energy.2015.02.038)
3. Coles DS, Blunden L, Bahaj AS. 2017 Assessment of the energy extraction potential at tidal sites around the Channel Islands. *Energy* **124**, 171–186. (doi:10.1016/j.energy.2017.02.023)
4. Bahaj AS, Myers L. 2004 Analytical estimates of the energy yield potential from the Alderney Race (Channel Islands) using marine current energy converters. *Renew. Energy* **29**, 1931–1945. (doi:10.1016/j.renene.2004.02.013)
5. Bailly du Bois PB, Dumas F, Solier L, Voiseux C. 2012 In-situ database toolbox for short-term dispersion model validation in macro-tidal seas, application for 2D-model. *Cont. Shelf Res.* **36**, 63–82. (doi:10.1016/j.csr.2012.01.011)
6. Thiebot J, du Bois PB, Guillou S. 2015 Numerical modeling of the effect of tidal stream turbines on the hydrodynamics and the sediment transport–application to the Alderney Race (Raz Blanchard), France. *Renew. Energy* **75**, 356–365. (doi:10.1016/j.renene.2014.10.021)
7. Guillou N, Neill SP, Robins PE. 2018 Characterising the tidal stream power resource around France using a high-resolution harmonic database. *Renew. Energy* **123**, 706–718. (doi:10.1016/j.renene.2017.12.033)

8. Polagye B, Thomson J. 2013 Tidal energy resource characterization: methodology and field study in Admiralty Inlet, Puget Sound, WA (USA). *Proc. Inst. Mech. Eng. A J. Power Energy* **227**, 352–367. (doi:10.1177/0957650912470081)
9. Liu *et al.* 2012. Q3
10. Milne *et al.* 2016.
11. Lewis MJ, Neill SP, Hashemi MR, Reza M. 2014 Realistic wave conditions and their influence on quantifying the tidal stream energy resource. *Appl. Energy* **136**, 495–508. (doi:10.1016/j.apenergy.2014.09.061)
12. Tatum SC, Frost CH, Allmark H, O'Doherty DM, Mason-Jones A, Prickett PW, Grosvenor RI, Byrne CB, O'Doherty T. 2016 Wave–current interaction effects on tidal stream turbine performance and loading characteristics. *Int. J. Mar. Energy* **14**, 161–179. (doi:10.1016/j.ijome.2015.09.002)
13. Prandtl L. 1925 Bericht¨uber Untersuchungen zur ausgebildeten Turbulenz. *Z. Angew. Math. Mech.* **5**, 136–139. (doi:10.1002/zamm.19250050212)
14. Von Kármán TH. 1931 Mechanical similitude and turbulence. Q3
15. Bowden KF. 1978 Physical problems of the benthic boundary layer. *Geophys. Survey* **3**, 255–296. (doi:10.1007/BF01449556)
16. Lueck RG, Lu Y. 1997 The logarithmic layer in a tidal channel. *Cont. Shelf Res.* **17**, 1785–1801. (doi:10.1016/S0278-4343(97)00049-6)
17. Soulsby R. 1997 *Dynamics of marine sands: a manual for practical applications*. Thomas Telford. Q4
18. Batten WMJ, Bahaj AS, Molland AF, Chaplin JR. 2008 The prediction of the hydrodynamic performance of marine current turbines. *Renew. Energy* **33**, 1085–1096. (doi:10.1016/j.renene.2007.05.043)
19. Gooch S, Thomson J, Polagye B, Meggitt D. 2009 Site characterization for tidal power. In OCEANS 2009, pp. 1–10. Q5
20. Thiebaut M, Sentchev A. 2017 Asymmetry of tidal currents off the W. Brittany coast and assessment of tidal energy resource around the Ushant Island. *Renew. Energy* **105**, 735–747. (doi:10.1016/j.renene.2016.12.082)
21. Lewis M, Neill SP, Robins P, Hashemi MR, Ward S. 2017 Characteristics of the velocity profile at tidal-stream energy sites. *Renew. Energy* **114**, 258–272. (doi:10.1016/j.renene.2017.03.096)
22. O'Rourke F, Boyle F, Reynolds A. 2014 Ireland's tidal energy resource; an assessment of a site in the Bulls Mouth and the Shannon Estuary using measured data. *Energy Convers. Manage.* **87**, 726–734. (doi:10.1016/j.enconman.2014.06.089)
23. Hagerman G, Polagye B, Bedard R, Previsic M. 2006 Methodology for estimating tidal current energy resources and power production by tidal in-stream energy conversion (TISEC) devices. *EPRI North American tidal in stream power feasibility demonstration project* 1. Q5
24. Bennis AC, Furgerot L, Bailly Du Bois P, Dumas F, Odaka T, Lathuilière C, Filipot J-F. 2019 Numerical modelling of three-dimensional wave-current interactions in complex environment: application to Alderney Race. *Appl. Ocean Res.* **95**, 102021. (doi:10.1016/j.apor.2019.102021)
25. Furgerot L, Bailly du Bois P, Méar Y, Poizot E, Morillon M. 2018 Velocity profile variabilities at a tidal-stream energy site (Raz Blanchard, France): from short (second) to yearly time scales. *OCEANS'18* MTS, Kobe. Q5
26. Furgerot L, Poprawski Y, Violet M, Poizot E, Bailly du Bois P, Morillon M, & Mear Y. 2019 High-resolution bathymetry of the Alderney Race and its geological and sedimentological description (Raz Blanchard, northwest France). *J. Maps* **15**, 708–718. (doi:10.1080/17445647.2019.1657510)
27. Lopez G, Bennis A-C, Barbin Y, Benoît L, Cambra R, Sentchev A. 2019 *Surface hydrodynamics of the Alderney Race from HF Radar Measurements*. In Proc. of the 13th European Wave and Tidal Energy Conf., Naples, Italy, Sep 2019. Q6
28. Thiebaut M, Sentchev A, Bailly du Bois P. 2019 Merging velocity measurements and modeling to improve understanding of tidal stream resource in Alderney Race. *Energy* **178**, 460–470. (doi:10.1016/j.energy.2019.04.171)
29. Legrand C. 2009 *Assessment of tidal energy resource: marine renewable energy guides*. European Marine Energy Centre. Q4
30. Bailly du Bois P, Pouderoux B, Dumas F. 2014 System for high-frequency simultaneous water sampling at several depths during sailing. *Ocean Eng.* **91**, 281–289. (doi:10.1016/j.oceaneng.2014.09.022)

31. Monin AS, Obukhov AM. 1954 Osnovnye zakonomernosti turbulentnogo peremeshivanija v prizemnom sloe atmosfery (Basic Laws of Turbulent Mixing in the Atmosphere Near the Ground). *Trudy geofiz. inst. AN SSSR* **24**, 163–187.
Q3 32. von Karman 1921.
33. Peterson EW, Hennessey Jr JP. 1978 On the use of power laws for estimates of wind power potential. *J. Appl. Meteorol.* **17**, 390–394. (doi:10.1175/1520-0450(1978)017<0390:OTUOPL>2.0.CO;2)
Q3 34. Myers, Bahaj 2009.
35. Iyer AS, Couch SJ, Harrison GP, Wallace AR. 2013 Variability and phasing of tidal current energy around the United Kingdom. *Renew. Energy* **51**, 343–357. (doi:10.1016/j.renene.2012.09.017)
36. Walters RA, Tarbotton MR, Hiles CE. 2013 Estimation of tidal power potential. *Renew. Energy* **51**, 255–262. (doi:10.1016/j.renene.2012.09.027)
37. Venugopal V *et al*. 2011 EquiMar.Deliverable D2. 2. Wave and tidal resource characterisation.
Q3 38. Tiebaut, Sentchev 2019.
39. Korotenko KA, Sentchev A. 2019 Estimates of turbulence intensity and power density of an asymmetric tidal current under wind forcing variability. *Izv. Atmos. Ocean. Phys.* **55**, 196–206. (doi:10.1134/S0001433819020099)
40. Goddijn-Murphy L, Woolf DK, Easton MC. 2013 Current patterns in the Inner Sound (Pentland Firth) from underway ADCP data. *J. Atmos. Ocean. Technol.* **30**, 96–111. (doi:10.1175/JTECH-D-11-00223.1)
41. Guerra M, Thomson J, Prusa T, Maloy CF, Krembs C, Sackmann B. 2019 Tidal current observations through Admiralty Inlet from ferry-mounted current profilers. *J. Ocean Eng. Mar. Energy* **5**, 159–172. (doi:10.1007/s40722-019-00135-w)
42. Thiébaut M, Filipot JF, Maisondieu C, Damblans G, Duarte R, Droniou E, Chaplain N, Guillou S. 2020 A comprehensive assessment of turbulence at a tidal-stream energy site influenced by wind-generated ocean waves. *Energy* **191**, 116550. (doi:10.1016/j.energy.2019.116550)
43. Thiebaut M, Sentchev A. 2016 Tidal stream resource assessment in the Dover Strait (eastern English Channel). *Int. J. Mar. Energy* **16**, 262–278. (doi:10.1016/j.ijome.2016.08.004)
44. Myers LE, Bahaj AS. 2010 Experimental analysis of the flow field around horizontal axis tidal turbines by use of scale mesh disk rotor simulators. *Ocean Eng.* **37**, 218–227. (doi:10.1016/j.oceaneng.2009.11.004)
45. Liu P, Veitch B. 2012 Design and optimization for strength and integrity of tidal turbine rotor blades. *Energy* **46**, 393–404. (doi:10.1016/j.energy.2012.08.011)
46. Milne IA, Day AH, Sharma RN, Flay RGJ. 2015 Blade loading on tidal turbines for uniform unsteady flow. *Renew. Energy* **77**, 338–350. (doi:10.1016/j.renene.2014.12.028)
47. Sentchev A, Thiébaut M, Schmitt FG. 2020 Impact of turbulence on power production by a free-stream tidal turbine in real sea conditions. *Renew. Energy* **147**, 1932–1940. (doi:10.1016/j.renene.2019.09.136)
48. MacEnri J, Reed M, Thiringer T. 2013 Influence of tidal parameters on SeaGen flicker performance. *Phil. Trans. R. Soc. A* **371**, 20120247. (doi:10.1098/rsta.2012.0247)
49. Lewis MJ, Palmer T, Hashemi R, Robins P, Saulter A, Brown J, Lewis H, Neill S. 2019 Wave-tide interaction modulates nearshore wave height. *Ocean Dyn.* **69**, 367–384. (doi:10.1007/s10236-018-01245-z)
50. Sentchev A, Yaremchuk M. 2016 Monitoring tidal currents with a towed ADCP system. *Ocean Dyn.* **66**, 119–132. (doi:10.1007/s10236-015-0913-z)
51. Sentchev A, Thiébaut M, Furgerot L, Bailly du Bois P, Morillon M. 2019 *Advances in resource characterization in Alderney Race (English Channel)*. In Proc. of the 13th European Wave and
Q6 Tidal Energy Conf., Naples, Italy, Sep 2019.